B-EXPRESS: A New Bounded EXtremum PREServing Strategy for Convective Schemes

M. Darwish and F. Moukalled*
Mechanical Engineering Department,
American University of Beirut
P.O.Box 11-0236
Beirut - Lebanon

Abstract

The indiscriminate application of the Convective Boundedness Criterion (CBC) in all flow regions results in a new and subtle error that leads to a significant reduction in accuracy at locations where physical extrema (maxima or minima) with steep profiles are present. In this paper, a new Bounded EXtremum PREServing Strategy (B-EXPRESS) that addresses this issue is presented. The B-EXPRESS is a two-stage procedure in which, an Extremum Recognition Algorithm (ERA) is first applied to a solution converged to a set level to flag locations at which enforcing the CBC leads to extrema attenuation. Then, in the second stage, an unbounded scheme is used at the flagged locations, while a bounded scheme is used elsewhere. The new strategy is applied to the SMART (a 3rd order bounded scheme) and BSEVENTH (a 7th order bounded scheme) schemes to yield two new schemes denoted by B-EXPRESS-3 and B-EXPRESS-7, respectively. These schemes are tested by solving four problems of pure convection in an oblique velocity field of a sinusoidal, elliptic, triangular, and box profiles. Results obtained reveal the B-EXPRESS-3 to greatly reduce the rate of attenuation in the levels of the profiles and to be as accurate as the BSEVENTH scheme which, on average, requires 540% more CPU time than the B-EXPRESS-3 scheme. Moreover, the B-EXPRESS-7 scheme computations do not show any observable attenuation in the levels of the profiles while marginally increasing the CPU effort (3.43% on average) over the BSEVENTH scheme.

^{*}Corresponding Author. Email: memouk@aub.edu.lb

Nomenclature

A Coefficients in the discretized equation.

B Source term integrated in the discretized equation.

C_f Convective flux coefficient.

Grad Gradient.

J Total scalar flux across cell face.

minGrad Minimum Gradient.

Q Source term in the conservation equation.

S Surface vector of cell face.

u Velocity vector.

 Γ Diffusion coefficient.

φ General dependent variable.

ρ Density.

ξ Local Curvilinear coordinate.

Superscripts

Refers to normalized variable.

C Convection contribution.

D Diffusion contribution.

U Upwind formulation.

Subscripts

C Central grid point.

D Downstream grid point.

E,W,. Refers to neighbors of the P grid point.

e,w,.. Refers to control volume faces.

f Refers to control volume face.

NB Refers to neighbours of the main grid point.

nb Refers to neighbours of a control volume face.

P Main grid point

U Upstream grid point.

Introduction

The numerical dispersion problems that have hindered the use of one-dimensional and multi-dimensional higher-order interpolation profiles in the simulation of convection-diffusion transport problems have been eliminated [1-4]. This has been accomplished by enforcing a monotonicity constraint or a Convective Boundedness Criterion (CBC) [5] on the higher-order profiles and has resulted in a family of bounded High Resolution schemes following either the TVD [6] or NVF/NVSF [1,7] approaches.

However, the indiscriminate application of the CBC in all flow regions has resulted in a new and subtle error that leads to a significant reduction in accuracy at locations where physical extrema (maxima or minima) with steep profiles are present. The reduction in accuracy is mainly due to the attenuation of the physical extrema levels. More specifically, the local physical extrema in the profiles gradually decrease in value with distance as if in the presence of a diffusion phenomenon.

This can be assessed in a very simple numerical experiment: simulation of pure convection of a sinusoidal, a triangular, an elliptic, or even a box profile using the SMART [5] or SHARP [1] scheme. As will be shown, prediction using the SMART scheme underestimate the maximum value by about 30% near the outlet region. On the other hand, employing an unbounded version of the SMART scheme, namely the QUICK scheme of Leonard [8], results in a much lower attenuation in the profile levels (~10% near the outlet). Moreover, results obtained with the BSEVENTH [9] scheme, a bounded Very High-Order scheme (Very High-Resolution) based on a seventh order profile, underestimate the maximum by about 10% near the outlet region, while the unbounded SEVENTH scheme yields negligible attenuation of the maximum. Even though the SEVENTH and QUICK schemes show lower attenuation levels, they suffer from a well known problem of over/under shoots which, for some problems, results in values for certain variables that are physically meaningless (e.g., negative density or energy).

This is a clear indication that significant improvements in accuracy can be achieved and unnecessary errors avoided if these extrema can be found and flagged in a computational field, and the CBC [5] de-activated at these locations while remaining active in the

remainder of the flow field, thus not compromising the boundedness of the solution profile. In his work on the explicit Non-oscillatory Integrally Reconstructed Volume-Averaged Numerical Advection scheme (NIRVANA) [10], Leonard addresses this issue and through the use of the "discrete integral variable", ψ , locates local extrema by inflection points in ψ . However, the ramifications of his approach have remained more-orless unnoticed by the computational fluid dynamics community at large. The underlying concepts are simple as will be demonstrated later, and his algorithm can be reformulated and fitted within a strategy that applies equally for implicit and explicit schemes in the scalar field. The development of such a strategy is the subject of this paper.

The Bounded EXtrema PREServing Strategy (B-EXPRESS) developed in this work to preserve extrema in steady flows, can be applied to the family of high-resolution schemes constructed using either the NVF/NVSF or the TVD methodology by incorporating a switch-off parameter that controls the application of the CBC. The strategy followed in implementing the B-EXPRESS is a two-stage procedure. In the first stage, an Extremum Recognition Algorithm (ERA) is applied to a solution converged to a set level obtained using a High-Resolution (HR) or Very High-Resolution (VHR) scheme to flag the extrema regions. Then, in the second stage, the computational field is driven to full convergence by using the unbounded base scheme in the flagged regions and the bounded scheme in the remainder of the domain. The B-EXPRESS is applied to the SMART and BSEVENTH schemes to yield two new schemes denoted by B-EXPRESS-3 and B-EXPRESS-7, respectively. Moreover, the new strategy is tested for efficiency and accuracy by comparing the performance, in four steady test problems, of the newly developed B-EXPRESS schemes against that of the SEVENTH, BSEVENTH, SMART, and QUICK schemes. Results indicate that accuracy similar to that of the BSEVENTH scheme is achieved with only about 70% increase in computational cost when compared to the SMART scheme and over 5 fold reduction when compared to the BSEVENTH scheme. It should be mentioned here that a fifth order scheme could have been chosen instead of the seventh order scheme. However, experimentation showed that the difference in results between the third and fifth order schemes is not as large as the difference between the third and seventh order schemes. Accordingly, the latter was chosen. Nevertheless, the methodology developed is applicable to all HR and VHR schemes irrespective of their order of accuracy.

In the remainder of this article, a brief description of the discretization process and the CBC is given followed by a short review of the high-resolution schemes used in this work. Then the ERA is presented and its implementation within the B-EXPRESS detailed. Finally, a number of problems are solved to illustrate the advantages of the new strategy.

Numerical Discretization of the Transport Equation

The transport equation governing two dimensional incompressible steady flows may be expressed in the following general form:

$$\nabla \cdot (\rho \mathbf{u} \phi) = \nabla \cdot (\Gamma \nabla \phi) + Q \tag{1}$$

where ϕ is any dependent variable, \mathbf{u} is the velocity vector, and ρ , Γ , and Q are the density, diffusivity, and source term respectively. Since a control volume based formulation is sought, Eq. (1) is integrated over the control volume shown in Figure 1(a) to yield, upon applying the divergence theorem, the following discretized equation:

$$J_e + J_w + J_n + J_s = B \tag{2}$$

where J_f represents the total flux of ϕ across cell face f (f= e, w, n or s), and B is the volume integral of the source term Q. Each of the surface fluxes J_f contains a convective contribution, J_f^C , and a diffusive contribution, J_f^D , hence:

$$\mathbf{J}_{\mathbf{f}} = \mathbf{J}_{\mathbf{f}}^{\mathbf{C}} + \mathbf{J}_{\mathbf{f}}^{\mathbf{D}} \tag{3}$$

where the diffusive flux is given by:

$$\mathbf{J}_{f}^{D} = \left(-\Gamma \nabla \phi\right)_{f} \mathbf{S}_{f} \tag{4}$$

and the convective flux by:

$$\mathbf{J}_{f}^{C} = (\rho \mathbf{u}.\mathbf{S})_{f} \, \phi_{f} = C_{f} \phi_{f} \tag{5}$$

where S_f is the surface of cell face f, and C_f is the convective flux coefficient at cell face f. The discretization of the diffusive flux does not require any special consideration and the use of a linear interpolation profile to write the gradient as a function of the neighboring grid points is adequate. Therefore, the suggested diffusion model is second-order accurate as would be the overall scheme in a diffusion-controlled problem.

The discretization of the convective flux is, however, problematic and requires special attention. As can be seen from Eq. (5), the accuracy of the control volume solution for the convective scalar flux depends on the proper estimation of ϕ_f as a function of the neighboring ϕ node values. Using some assumed interpolation profile, ϕ_f can be explicitly formulated by a functional relationship of the form:

$$\phi_{f} = f(\phi_{nb}, C_{f}) \tag{6}$$

where ϕ_{NB} denotes the neighboring ϕ node values (ϕ_E , ϕ_W , ϕ_N , ϕ_S , ϕ_P , ϕ_{EE} , ϕ_{WW} , ϕ_{NN} , ϕ_{SS} , etc...). The interpolation profile may be one-dimensional or multi-dimensional of low or high-order of accuracy. The higher the order of the profile is, the lower numerical diffusion will be. However, the order of the profile and its dimensionality do not eliminate over/undershoots. As explained later, this error is minimized by forcing the convective flux to remain within set bounds.

After substituting the face values by their functional relationships relating to the node values of ϕ , Eq. (2) is transformed after some algebraic manipulations into the following discretized equation:

$$A_{P}\phi_{P} = \sum_{NB} A_{NB}\phi_{NB} + B_{P} \tag{7}$$

where the coefficients A_P and A_{NB} depend on the selected scheme and B_P is the source term of the discretized equation. An equation similar to Eq. (7) is obtained at every grid point in the domain and the collection of all these equations form a system of algebraic equations that is solved here iteratively to obtain the ϕ field.

Normalized Variables and the Convection Boundedness Criterion (CBC)

As mentioned above, to minimize the numerical dispersion error, limiters on the convective flux should be imposed. The flux limiter denoted by the CBC [5] is adopted here and explained next in terms of the normalized variables approach. Figure 1(b) shows the local behavior of the convected variable near a control-volume face. If the value of the

dependent variable at the control volume face located at a distance ξ_f from the origin is expressed by ϕ_f , then the normalized variables (Figures 1(c)) will be defined as [7]:

$$\widetilde{\phi} = \frac{\phi - \phi_{U}}{\phi_{D} - \phi_{U}}$$

$$\widetilde{\xi} = \frac{\xi - \xi_{U}}{\xi_{D} - \xi_{U}}$$
(8)

where the subscripts U and D that depend on the flow direction, refer to upstream and downstream locations, respectively.

Using the normalized variables, the CBC for implicit steady state flow calculations [5], states that for a scheme to have the boundedness property its functional relationship should be continuous and bounded from below by $\Phi_f = \Phi_C$ and from above by unity, should pass through the point (0,0) and (1,1) in the monotonic range $0 < \Phi_C < 1$, and for $\Phi_C < 0$ or $\Phi_C > 1$ the functional relationship $f(\Phi_C)$ should equal Φ_C . These conditions can be described graphically on a Normalized Variable Diagram (NVD) as shown in Fig. 2.

This criterion can be imposed on any scheme, irrespective of the order of its interpolation profile. It will be used to ensure the boundedness of the third and seventh order schemes described below.

Higher-Order Schemes

The CBC can currently be enforced on any interpolation profile in order to get its equivalent bounded version. In general, an interpolation profile can be constructed by fitting a polynomial, as in the following equation, to a set of control volume nodes judiciously chosen (Fig. (3a)):

$$\phi = a_0 + a_1 \xi + a_2 \xi^2 + a_3 \xi^3 + a_4 \xi^4 + a_5 \xi^5 + \dots$$
 (9)

In the above equation (Eq. (9)), ξ represents the local coordinate axis. The order of the polynomial can be chosen to yield the required scheme with its coefficients calculated by fitting the polynomial to a number of nodes in the computational domain. Since the new strategy developed in this work is tested using a third and a seventh order schemes, attention is focussed on the polynomial profiles used in constructing these schemes. The unbounded third order scheme, denoted by QUICK [8] can be constructed by fitting a

second order polynomial to the nodes at locations U, C, and D (Figure 3(b)). The resulting functional relationship for the QUICK scheme may be written for a regular grid as:

$$\phi_{\rm f} = \frac{3}{8}\phi_{\rm D} + \frac{3}{4}\phi_{\rm C} - \frac{1}{8}\phi_{\rm U} \tag{10}$$

and for an irregular grid as:

$$\phi_{f} = \frac{\prod_{\substack{nb \neq D}} (\xi_{f} - \xi_{NB})}{\prod_{\substack{nb \neq D}} (\xi_{D} - \xi_{NB})} \phi_{D} + \frac{\prod_{\substack{nb \neq C}} (\xi_{f} - \xi_{NB})}{\prod_{\substack{nb \neq C}} (\xi_{C} - \xi_{NB})} \phi_{C} + \frac{\prod_{\substack{nb \neq U}} (\xi_{f} - \xi_{NB})}{\prod_{\substack{nb \neq U}} (\xi_{U} - \xi_{NB})} \phi_{U}$$
(11)

Similarly, the unbounded seventh order scheme can be built by fitting a 6th order polynomial to the nodes at locations UUU, UU, U, C, D, DD, DDD (Figure 3(c)). Its functional relationship over a regular grid is given by:

$$\phi_{\rm f} = \frac{7}{1024} \phi_{\rm DDD} - \frac{35}{512} \phi_{\rm DD} + \frac{525}{1024} \phi_{\rm D} + \frac{175}{256} \phi_{\rm C} - \frac{175}{1024} \phi_{\rm U} + \frac{21}{512} \phi_{\rm UU} - \frac{5}{1024} \phi_{\rm UUU}$$
(12)

and over an irregular grid by:

$$\phi_{f} = \frac{\prod_{\substack{nb \neq DDD \\ nb \neq DDD}} (\xi_{f} - \xi_{nb})}{\prod_{\substack{nb \neq DD \\ nb \neq DDD}} (\xi_{DDD} - \xi_{nb})} \phi_{DDD} + \frac{\prod_{\substack{nb \neq DD \\ nb \neq DD}} (\xi_{DD} - \xi_{nb})}{\prod_{\substack{nb \neq DD \\ nb \neq DD}} (\xi_{D} - \xi_{nb})} \phi_{DD} + \frac{\prod_{\substack{nb \neq DD \\ nb \neq DD}} (\xi_{DD} - \xi_{nb})}{\prod_{\substack{nb \neq DD \\ nb \neq DD}} (\xi_{D} - \xi_{nb})} \phi_{D} + \frac{\prod_{\substack{nb \neq DD \\ nb \neq DD}} (\xi_{f} - \xi_{nb})}{\prod_{\substack{nb \neq DD \\ nb \neq UU}} (\xi_{f} - \xi_{nb})} \phi_{UU} + \frac{\prod_{\substack{nb \neq UU \\ nb \neq UU}} (\xi_{UU} - \xi_{nb})}{\prod_{\substack{nb \neq UUU \\ nb \neq UU}} (\xi_{UU} - \xi_{nb})} \phi_{UU} \tag{13}$$

The bounded versions of the QUICK (known in the literature by SMART [5]) and seventh order schemes (denoted by SEVENTH) are obtained by simply using Eqs. (10)-(13) to calculate the value of ϕ at the control volume face, normalizing ϕ_C and ϕ_f to yield ϕ_C and ϕ_f respectively, and then enforcing the CBC in the event it is not satisfied. The resultant ϕ_f is subsequently unnormalized to yield the bounded value of ϕ_f .

The Extremum Recognition Algorithm (ERA)

As illustrated in Figure 4, an Extremum Recognition Algorithm (ERA) should be based on the fact that a local extremum is characterized by a change of the gradient sign before and after its location. Using this property, it is conceptually possible to determine the location of any extremum in a scalar field by calculating the gradients and searching for a sign change. However, two difficulties arise within the context of a numerical solution. Even though the roots of these difficulties are different, their outcome is the same namely the creation of artificial extrema. The first is caused by pseudo-time numerical oscillations around a certain value arising from round-off errors or from iterative solutions that are not fully converged, whereas the second is due to the unphysical behavior of unbounded convective schemes (dispersion error), and guarding against these two pitfalls is important. In this work, the first difficulty is addressed by the ERA while the second is anticipated by the B-EXPRESS.

Since the CBC is enforced on a control volume surface basis, it is only needed to restrict attention to locating extremum within a computational cell. Figure 4 illustrates the various possible configurations that may arise in the ERA. In all cases, the gradients at the control volume faces (Grad^w, Grad^e,...) are calculated and their absolute values compared to a set value "minGrad" (=0.05). If the absolute values of the gradients are larger than "minGrad" and the gradients have opposite signs (Figure 4(a)), then a local maximum is present within the control volume and the two surfaces are flagged. If the value of the gradient at one of the surfaces is less than "minGrad" (the other value being higher), then the gradient on the surface of the adjacent cell is calculated and its value compared to "minGrad" (Figure 4(b)), or Figure 4(c)). If the two gradients have opposite signs then a local extremum is estimated to be present in the adjacent control volume and only the surface in question is flagged. The configurations depicted in Figures 4(d) and 4(e) are covered by the one shown in Figure 4(a) and therefore do not require any attention. This simple algorithm can also be applied with the appropriate sign change to locating local minima. Mathematically the algorithm is written as:

$$\begin{cases} \operatorname{Grad}_{i}^{w} >> 0 >> \operatorname{Grad}_{i}^{e} \| \operatorname{Grad}_{i}^{w} << 0 << \operatorname{Grad}_{i}^{e} \Rightarrow \operatorname{flag} \to w, e \\ \operatorname{Grad}_{i}^{ww} >> 0 >> \operatorname{Grad}_{i}^{e} \| \operatorname{Grad}_{i}^{ww} << 0 << \operatorname{Grad}_{i}^{e} \Rightarrow \operatorname{flag} \to w \end{cases}$$

$$(14)$$

$$\operatorname{Grad}_{i}^{w} >> 0 >> \operatorname{Grad}_{i}^{ee} \| \operatorname{Grad}_{i}^{w} << 0 << \operatorname{Grad}_{i}^{ee} \Rightarrow \operatorname{flag} \to e$$

The ">>0" sign indicates that "Grad" is larger in magnitude than "minGrad" and positive, while the "0<<" sign indicates that the "Grad" is larger in magnitude than "minGrad" and negative.

The above-described procedure is not limited to situations in which the convected variable is of order unity, rather, it is applicable to convected variables of any order of magnitude. This is true because the algorithm is based on the change in the sign of the gradient rather than its magnitude.

The Bounded EXtrema PREServing Strategy (B-EXPRESS)

With the ERA defined, its implementation within the iteration cycles of the overall CFD program is now described. Bearing in mind the second issue that need to be addressed by the B-EXPRESS, namely the suppression of local extrema originating from dispersion error, it was decided to implement the B-EXPRESS in two steps similar and compatible with the adaptive stencil strategy of Darwish and Moukalled [9]. In the first step a near converged solution is obtained using a bounded high-resolution scheme to ensure that undue oscillations are removed before using the ERA for flagging. The ERA is then invoked to determine the control volume faces that should be flagged, and the nearly converged field is driven to full convergence using a modified HR scheme whereby the CBC is enforced only on the non-flagged cell sides. Because the solution is nearly converged, the number of iterations needed to reach full convergence and thus the computational cost are minimized. Therefore, the ERA is employed once during the global iteration cycle to define the flagged region of a bounded nearly converged solution.

Filtering of Plateau Regions

In certain situations where a plateau exists (Fig. 5), the application of the current strategy can yield inaccurate results due to a steepening of the profiles. This situation is illustrated in the fourth test problem where a box profile is convected. The ERA algorithm flags a

number of control volumes on both sides of the steep section of the box profile. This flagging is due to the fact that the used solution is not complete and contain some numerical diffusion which changes the profile from a plateau section into a round section. This detrimental behavior is easily corrected in the B-EXPRESS methodology through the use of a filtering algorithm which turns off the ERA flagging whenever proportion of the gradient magnitudes on both sides of an extrema exceeds a value of 5 i.e. whenever one of the gradients has a magnitude 5 times larger than the gradient on the other side.

Results and Discussion

To demonstrate the virtues of the new strategy, four problems involving convection in an oblique velocity field of the following profiles are considered: a sinusoidal profile (Fig. 6(a)), a triangular profile(Fig. 6(b)), an elliptic profile (Fig. 6(c)), and a box profile (Fig. 6(d)). Results are obtained by covering the computational domains with uniform grids of sizes 20x20. Grid networks are generated using the Transfinite Interpolation technique [11]. In all tests, computational results are considered converged when the residual error (ERROR) defined as:

$$ERROR = \underset{i=1}{\text{MAX}} \left| A_p \phi_p - \left(\sum_{NB} A_{NB} \phi_{NB} + B_p \right) \right|$$
 (15)

becomes smaller than 10^{-5} .

Accuracy of the B-EXPRESS

Convection of a sinusoidal profile in an oblique velocity field

Figure 6(a) shows the first benchmark test problem consisting of a pure convection of a sinusoidal profile imposed at the inflow boundaries of a square computational domain. The sinusoidal profile is generated using the following equation:

$$\phi = \sin\left(\frac{i\pi}{L_i}\right) \qquad 1 \le i \le 10 \qquad \text{and} \qquad L_i = 5 \tag{16}$$

The results obtained using a number of schemes are depicted in Fig. 7. As shown, profiles are displayed at three different axial stations, near the inlet (x=0.375), near the centerline (x=0.525), and near the outlet (x=0.775) of the domain. It can be clearly seen that the

profiles obtained using the SMART and BSEVENTH schemes have a decreasing maxima as the flow moves towards the outlet region. This behavior resembles a diffusion-like phenomenon and should not be present in a pure convective situation. The unbounded version of SMART and BSEVENTH schemes, namely the QUICK and SEVENTH schemes, have better physical extrema preserving properties. The QUICK scheme results are similar to those of the BSEVENTH scheme in spite of the difference in the order of their interpolation profiles (3rd versus 7th). The SEVENTH scheme computation does not show any observable attenuation in the profile. However, both unbounded schemes (QUICK and SEVENTH) show unphysical oscillations which are detrimental to the overall accuracy. The B-EXPRESS-3 and B-EXPRESS-7, which are the schemes obtained by applying the ERA procedure to the SMART and BSEVENTH schemes, have profiles that are similar to those of the unbounded schemes but without unphysical oscillations. This is a clear indication of the effectiveness of the developed strategy. Moreover, the increase in accuracy of the B-EXPRESS schemes over their original counterparts is over 12% at x=0.775.

Convection of a triangular profile in an oblique velocity field

A triangular profile is used for the same geometric situation. This second test, illustrated in Figure 6(b), is more stringent than the sinusoidal test because of its sharp maximum. The triangular profile is generated using the following equation:

$$\phi = \begin{cases} \frac{i-1}{L_{i}} & 1 \le i \le 5\\ \frac{-(i-9)}{L_{i}} & 5 \le i \le 9 \end{cases}$$
 and $L_{i} = 4$ (17)

The trends of results, shown in Fig. 8, are similar to those reported in Fig.7. The SMART and BSEVENTH schemes show significant attenuation in the profiles as the flow moves towards the outlet. The B-EXPRESS-3 predictions are similar to the BSEVENTH results despite the difference in the order of their interpolation profiles. The B-EXPRESS-7 results do not show any observable attenuation of the extrema, which indicates an excellent performance. Moreover, at x=0.775, the B-EXPRESS-3 profile is about 8% more

accurate than that obtained using SMART and the B-EXPRESS-7 profile is over 12% more accurate than that generated by the BSEVENTH scheme.

Convection of an elliptic profile in an oblique velocity field

The B-EXPRESS was also tested for an elliptic profile (Fig. 6(c)) generated using the following equation:

$$\phi = \sqrt{1 - \frac{(i - 6)^2}{(L_i)^2}} \qquad 1 \le i \le 11 \quad \text{and} \quad L_i = 5$$
 (18)

Results obtained via the QUICK, SEVENTH, SMART, BSEVENTH, B-EXPRESS-3, and B-EXPRESS-7 are displayed in Fig. 9. As for the previous two problems, profiles at three different locations are presented (x=0.375, x=0.525, and x=0.775). The trend of results is consistent with what was obtained in the previous two test problems and shows the new strategy to be effective in decreasing the rate of attenuation in the profiles. As before, the best bounded results are obtained when using the B-EXPRESS-3 and B-EXPRESS-7, with profiles generated with the B-EXPRESS-3 (a third order scheme) being of quality similar to those obtained with the BSEVENTH (a seventh order scheme). Moreover, results obtained with B-EXPRESS-7 do not show any observable attenuation in the extrema. Again, as compared to the base schemes, the new B-EXPRESS schemes increase the accuracy by about 10% at x=0.775.

Convection of a box profile in an oblique velocity field

The last problem deals with the convection of a box profile in an oblique velocity field. The physical situation for this problem is shown in Fig. 6(d). This profile is chosen to test the B-EXPRESS strategy in the existence of a plateau region. The box profile at inlet to the domain is defined by:

$$\phi = \begin{cases} 1 & 1 \le i \le 5 \text{ and } 1 \le j \le 5 \\ 0 & \text{elsewhere} \end{cases}$$
 (19)

Profiles at two different streamwise locations (x=0.25 and x=0.75) are presented (Fig. 10). The filtering of the plateau region using the previously described strategy seems to be working well with no signs to any problems. The unboundedness of QUICK and SEVENTH is obvious. The attenuation in the maxima levels is almost eliminated with both

B-EXPRESS schemes and the overall trend of results is identical to that obtained in the previous test problems. Improvements with B-EXPRESS-3 over SMART (12% at x=0.75) are more pronounced than B-EXPRESS-7 over BSEVENTH due to a better performance of the BSEVENTH scheme in this problem.

Efficiency of the B-EXPRESS

In the above sections, the increase in accuracy with the B-EXPRESS was shown. The question arises, however, as to whether this increase in accuracy is associated with a high increase in computational cost or not. To eliminate doubts, the CPU times needed to solve the above-mentioned problems using the various schemes are displayed in Fig. 11. The trend is similar for the various profiles. The increase in computational cost with B-EXPRESS-3 is about 70% over SMART. However, the accuracy is the same as that achieved with the BSEVENTH scheme which needs 540% the CPU effort needed by B-EXPRESS-3 (Figs. 11(a)-(d)). Moreover, the increase in CPU time with B-EXPRESS-7 is marginal as compared to BSEVENTH (3.43% on average, Figs. 11(a), 11(c), and (d) show a slight increase whereas Fig. 11(b) shows a decrease). Keeping in mind the higher accuracy of the B-EXPRESS-7, it is more efficient to be used, since for a desired level of accuracy, a denser grid will be needed with the BSEVENTH scheme.

Concluding Remarks

A general strategy for the development of extrema-preserving schemes has been presented and applied to a bounded third order scheme (SMART) and a bounded seventh order scheme (BSEVENTH) to yield two new schemes denoted by B-EXPRESS-3 and B-EXPRESS-7, respectively. The new schemes were tested by solving four purely steady convective transport problems. The ERA based schemes (B-EXPRESS-3 and B-EXPRESS-7) showed significant decrease in the attenuation of the extrema in all tests, with the B-EXPRESS-7 computation not showing any observable preservation of the extrema throughout the computational domain. These improvements were obtained without oscillations since the CBC is still applied where needed. Moreover, The B-EXPRESS-3 results were found to be as accurate as the BSEVENTH results with the latter

requiring, on average, 540% more CPU effort. On the other hand, predictions using the B-EXPRESS-7 scheme did not show any observable attenuation in the levels of the profiles while requiring, on average, 3.43% more time than the BSEVENTH scheme.

Acknowledgments

The financial support provided by the University Research Board of the American University of Beirut is gratefully acknowledged.

References

- 1. Leonard, B.P., "Simple High Accuracy Resolution Program for Convective Modeling of Discontinuities," Int. J. Num. Methods Eng., vol. 8, pp. 1291-1319, 1988.
- Leonard, B.P., "The ULTIMATE Conservative Difference Scheme Applied to Unsteady One-dimensional Advection," Comp. Methods Applied Mech. Eng., vol. 88, pp. 17-74, 1991.
- 3. Darwish, M.S., "A Comparison of Six High Resolution Schemes Formulated Using the NVF Methodology," 33rd Science Week, Aleppo, Syria, 1993.
- 4. Moukalled, F. and Darwish, M.S., "A New Bounded-Skew Central Difference Scheme-Part I: Formulation and Testing", Num. Heat Transfer, Part B, vol. 31, pp. 91-110, 1996.
- 5. Gaskell, P.H. and Lau, A. K. C., "Curvature Compensated Convective Transport: SMART, A New Boundedness Preserving Transport Algorithm," Int. J. Num. Meth. Fluids, vol. 8, pp. 617-641, 1988.
- 6. Sweeby, P.K., "High Resolution Schemes Using Flux-Limiters for Hyperbolic Conservation Laws," SIAM J. Num. Anal., vol. 21, pp. 995-1011, 1984.
- Darwish, M.S. and Moukalled, F., "Normalized Variable and Space Formulation Methodology for High-Resolution Schemes," Num. Heat Trans., part B, vol. 26, pp. 79-96, 1994.
- 8. Leonard, B.P., "A Stable and Accurate Convective Modeling Procedure Based on Quadratic Interpolation," Comp. Methods Appl. Mech. & Eng., vol. 19, pp. 59-98, 1979.
- 9. Darwish, M. and Moukalled, F., "An Efficient Very High-Resolution scheme Based on an Adaptive-Scheme Strategy," Numerical Heat Transfer, Part B, vol. 34, pp. 191-213, 1998.
- 10. Leonard, B.P., Lock, A.P., and Macvean, M.K., "The NIRVANA Scheme Applied to One-dimensional Advection," Int. J. Num. Heat Fluid Flow, vol. 5, pp. 341-377, 1995.
- 11. Gordon, N.J. and Thiel, L.C., "Transfinite Mappings and Their Applications to Grid Generation," in Thompson, J.F. (ed.), Numerical Grid Generation, North-Holland, New York, pp. 171-192, 1982.

Figure Captions

- Figure 1: (a) Control volume, (b) convected variable near a control volume face, and (c) normalized variables.
- Figure 2: Normalized Variable Diagram (NVD).
- Figure 3: Interpolation Profiles.
- Figure 4: The ERA Algorithm.
- Figure 5: Filtering the plateau region.
- Figure 6: Pure convection of (a) a sinusoidal profile, (b) a triangular profile, (c) elliptic profile, (d) double-step profile.
- Figure 7: Convection of a sinusoidal profile at x=0.375, x=0.525, x=0.775.
- Figure 8: Convection of a triangular profile at x=0.375, x=0.525, x=0.775.
- Figure 9: Convection of an elliptic profile at x=0.375, x=0.525, x=0.775.
- Figure 10: Convection of a double-step profile at x=0.25, x=0.75.
- Figure 11: Time comparison for the convection in an oblique flow field of a (a) sine profile, (b) triangular profile, (c) elliptic profile, and (d) double step profile.

Figures

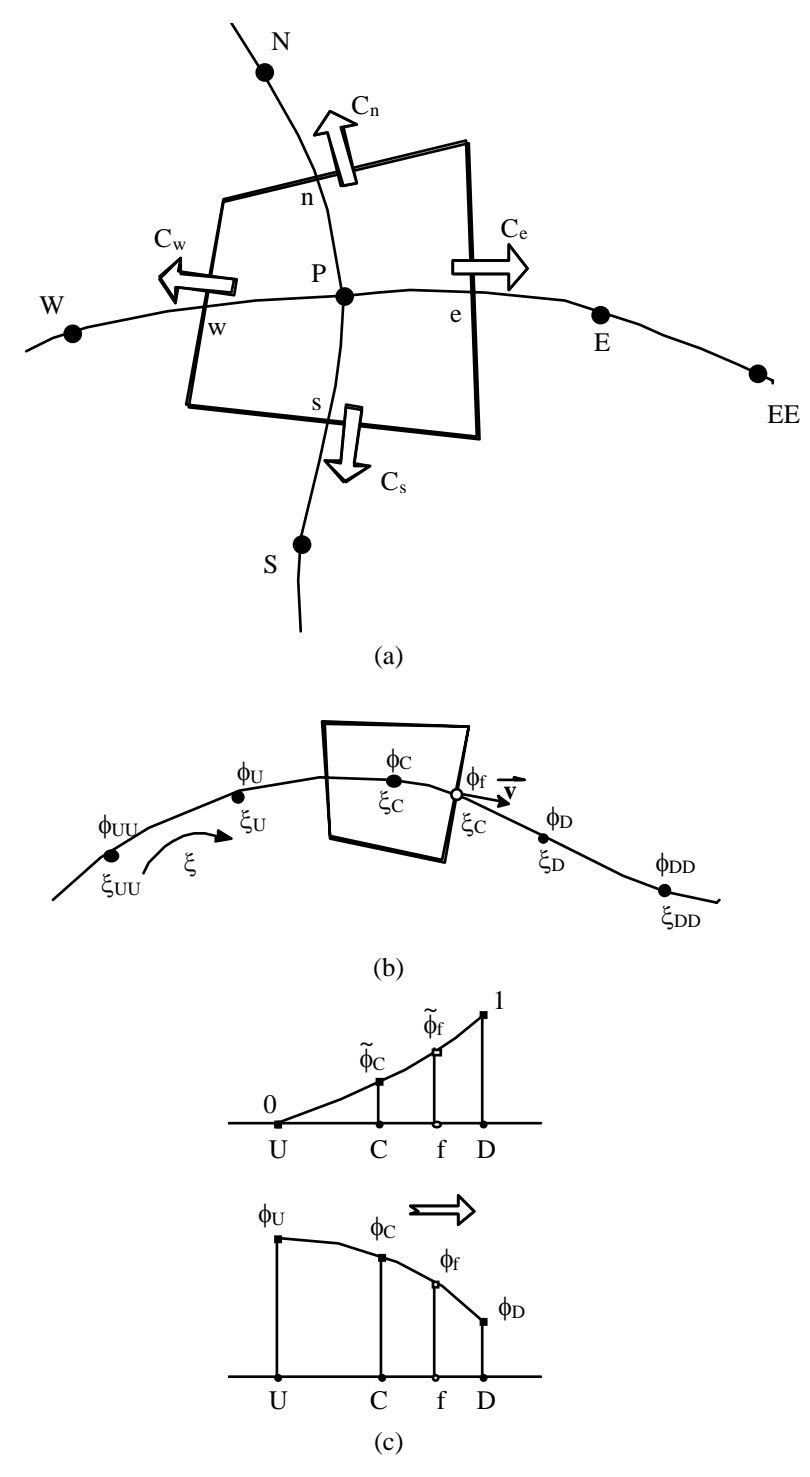


Figure 1: (a) Control volume, (b) convected variable near a control volume face, and (c) normalized variables.

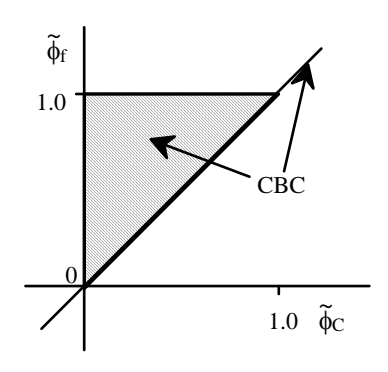
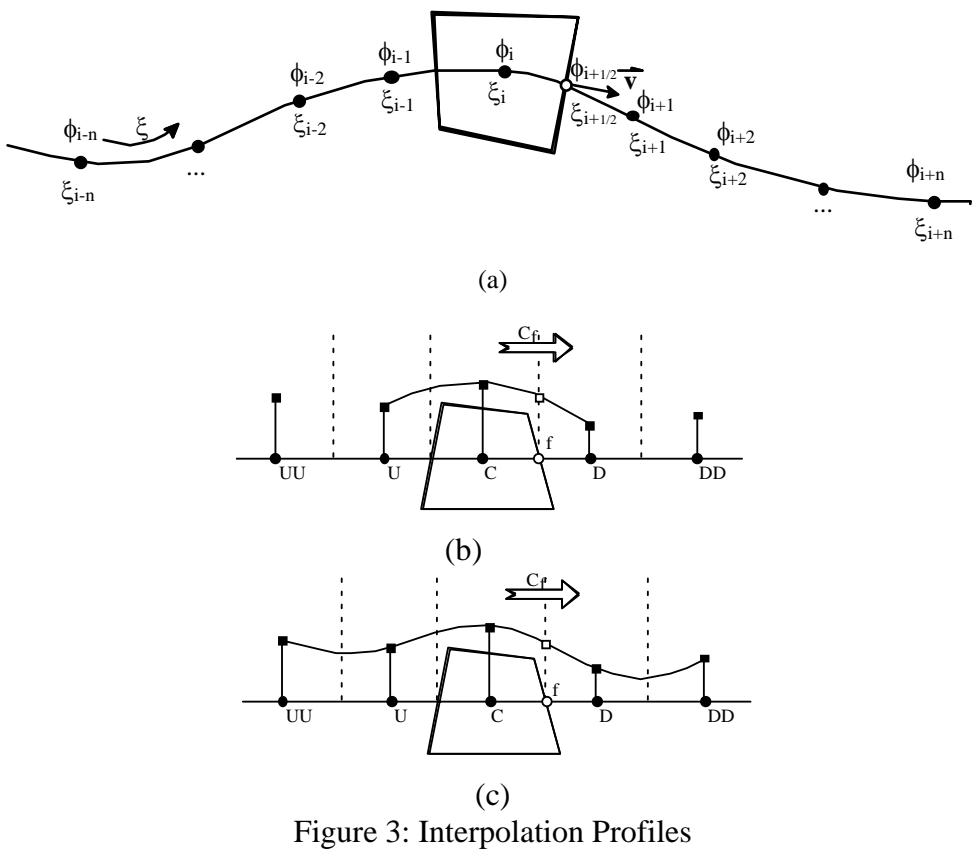


Figure 2: Normalized Variable Diagram (NVD).



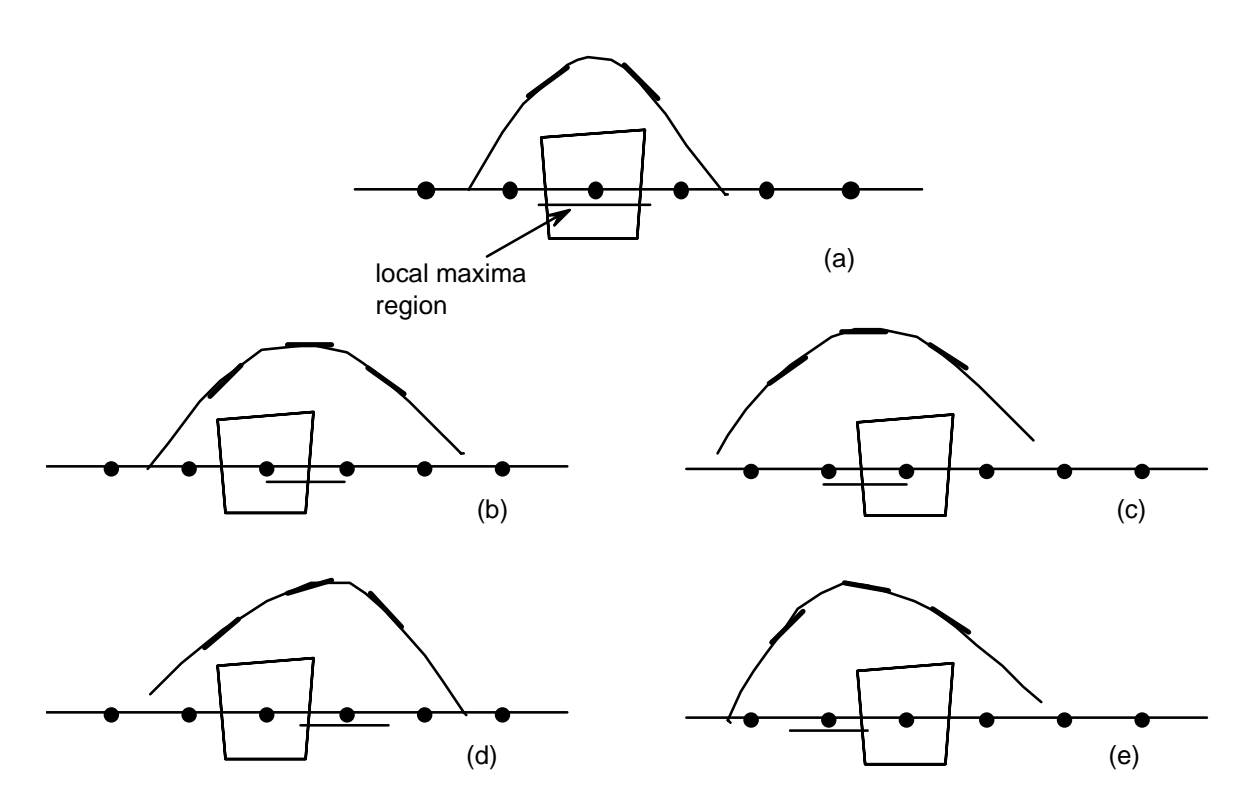


Figure 4 : The ERA Algorithm.

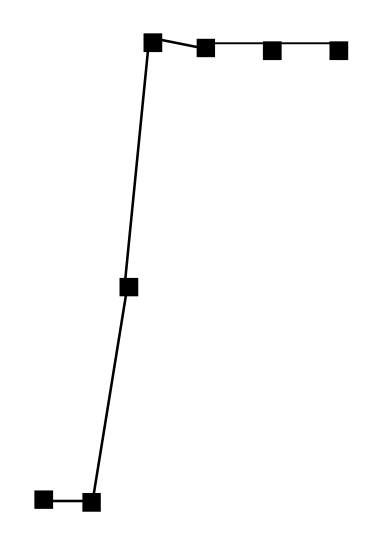


Figure 5: Filtering the plateau region.

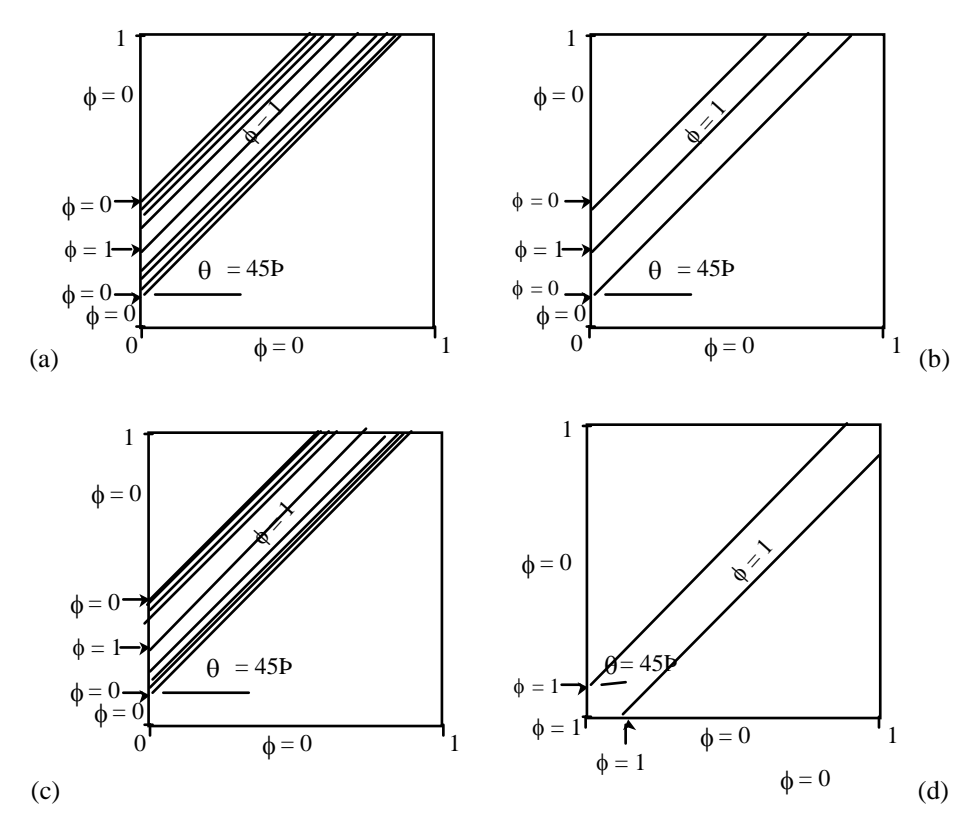
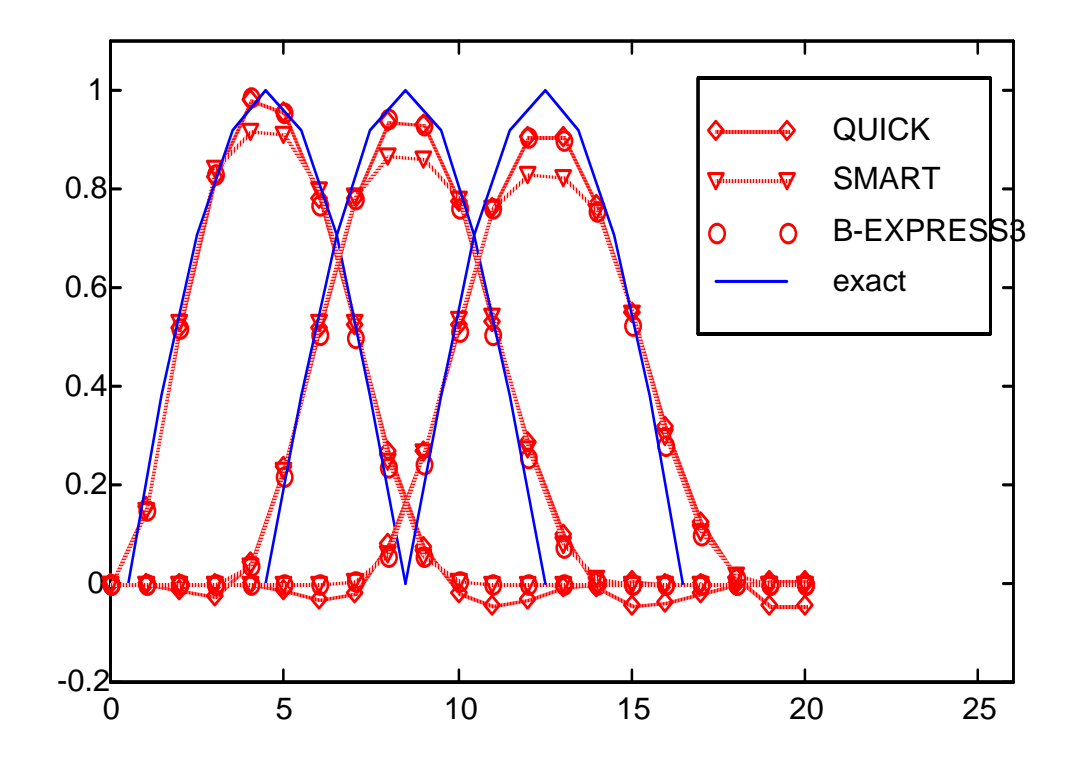


Figure 6: Pure convection of (a) a sinusoidal profile, (b) a triangular profile, (c) elliptic profile, (d) double-step profile.



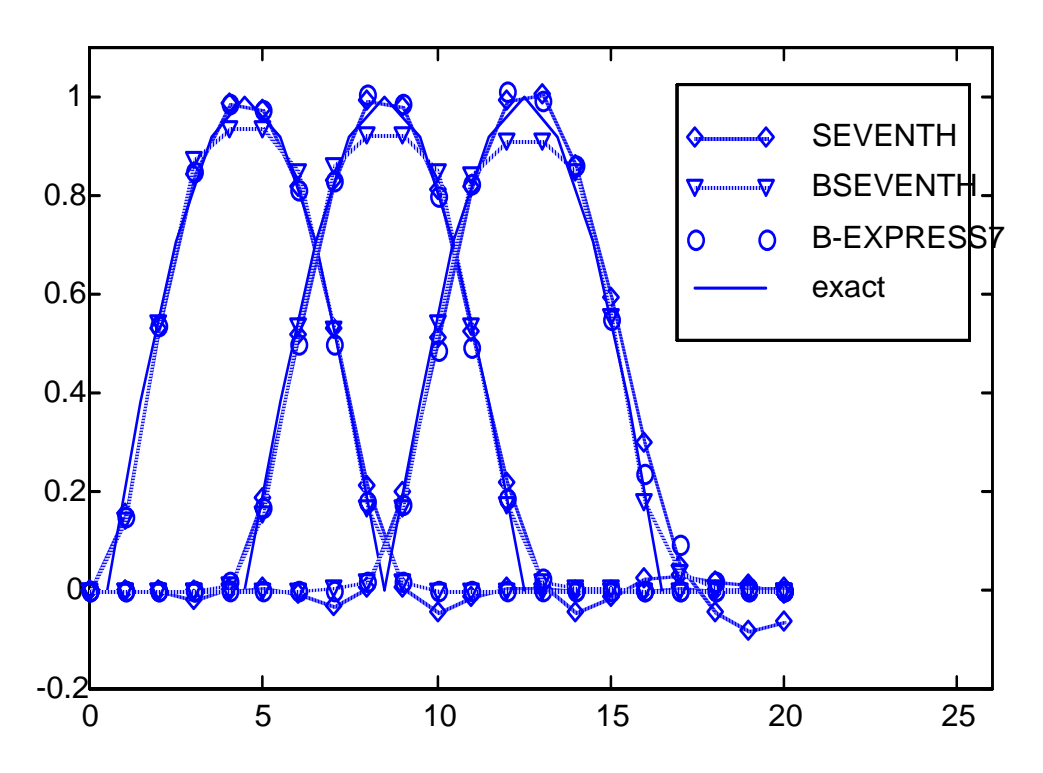
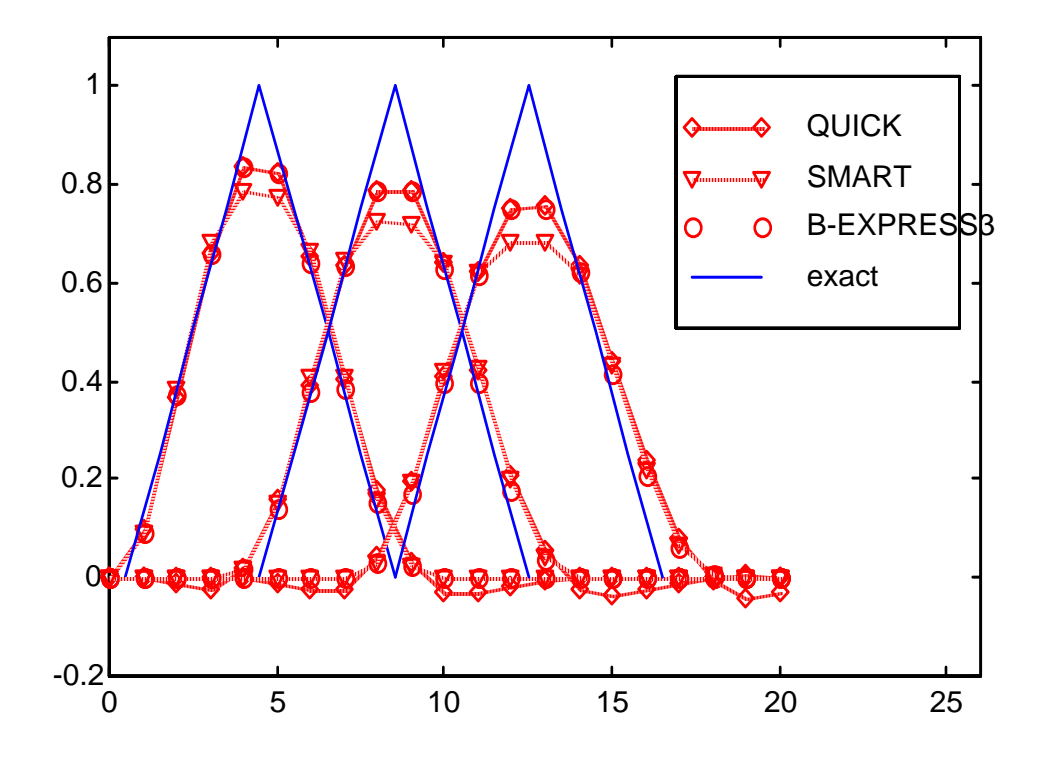


Figure 7: Convection of a sinusoidal profile at x=0.375, x=0.525, x=0.775.



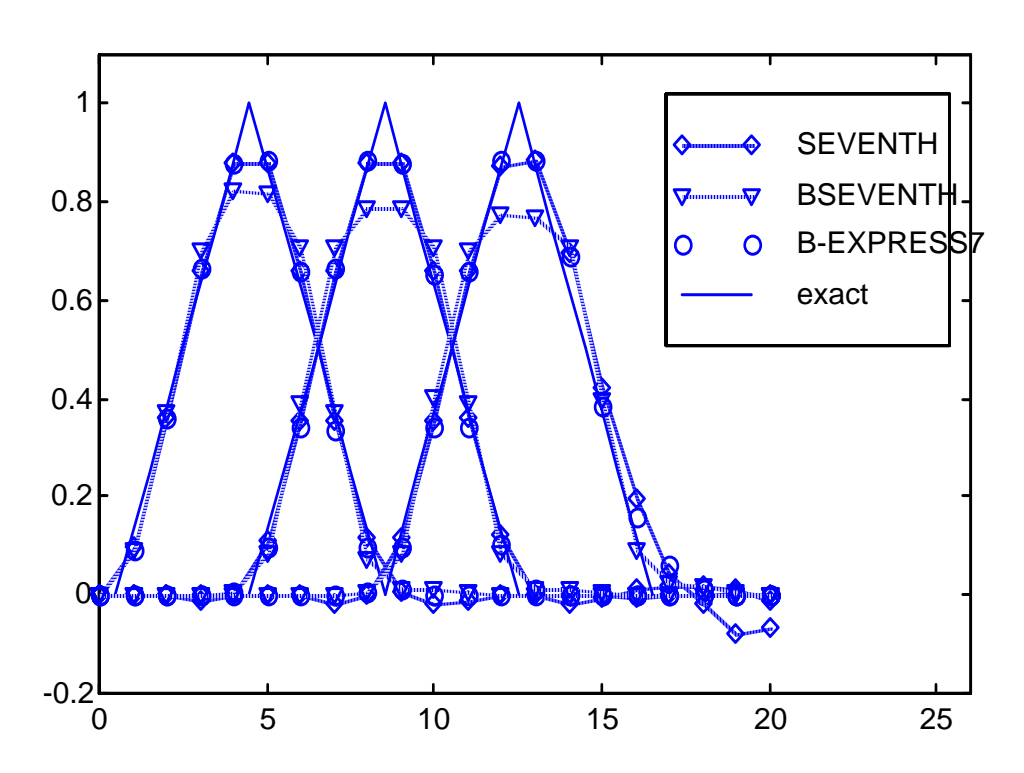
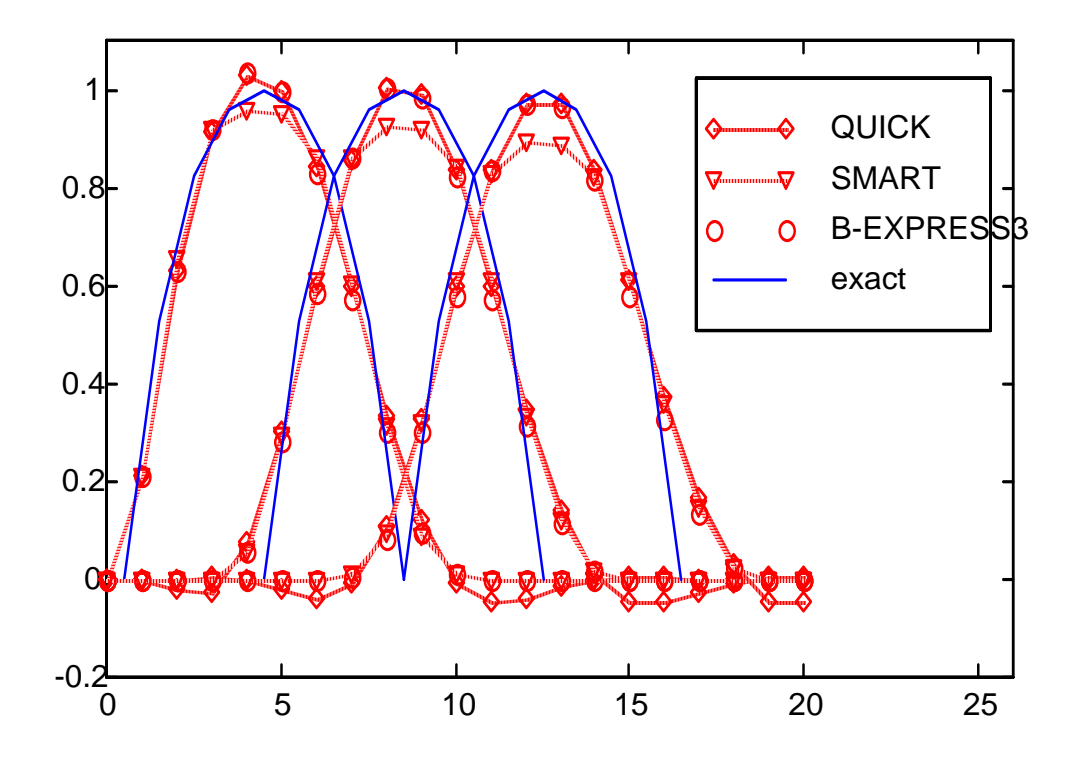


Figure 8: Convection of a triangular profile at x=0.375, x=0.525, x=0.775.



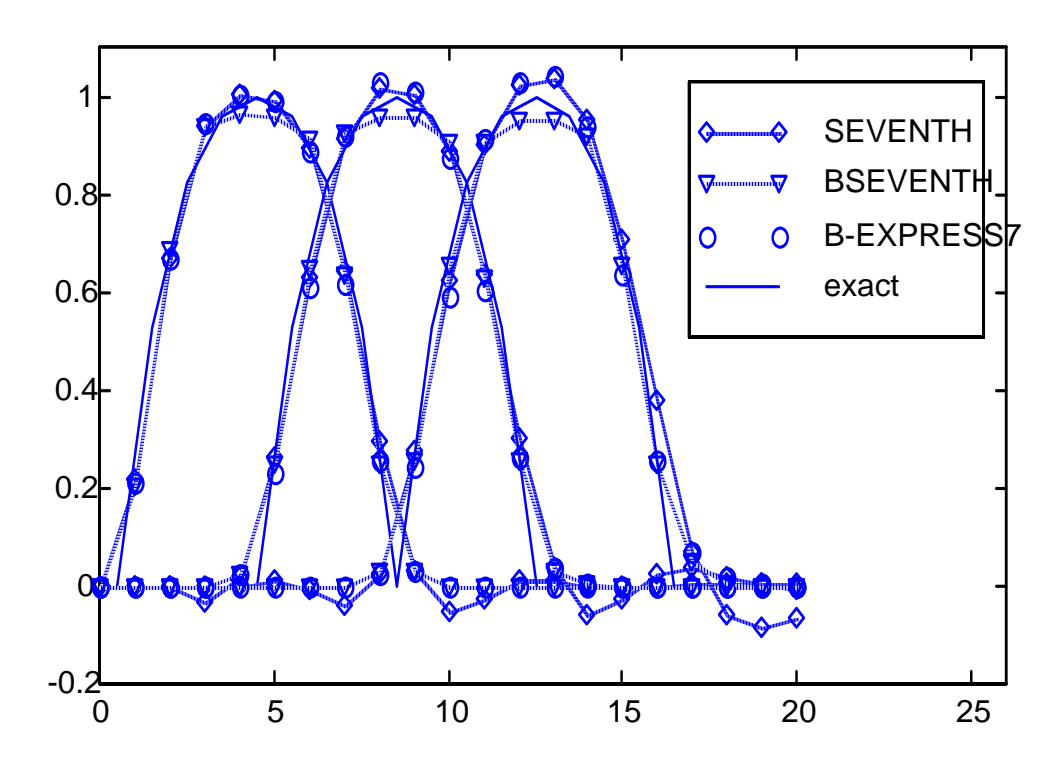
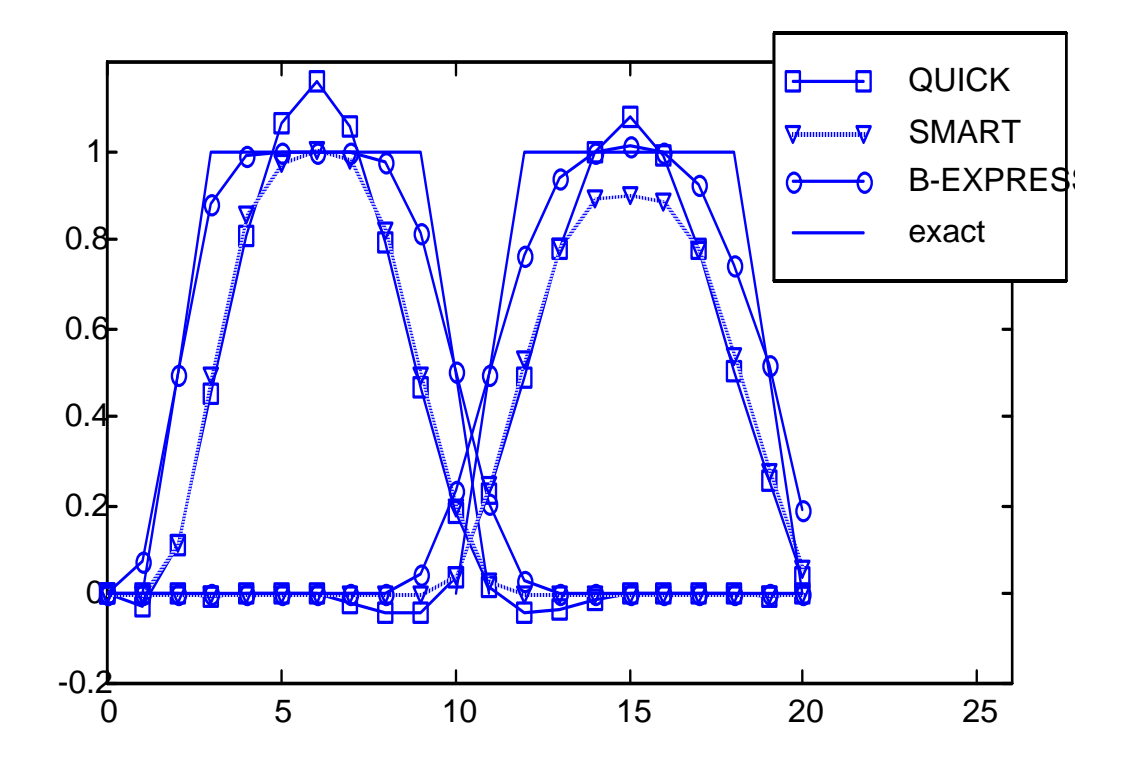


Figure 9: Convection of an elliptic profile at x=0.375, x=0.525, x=0.775.



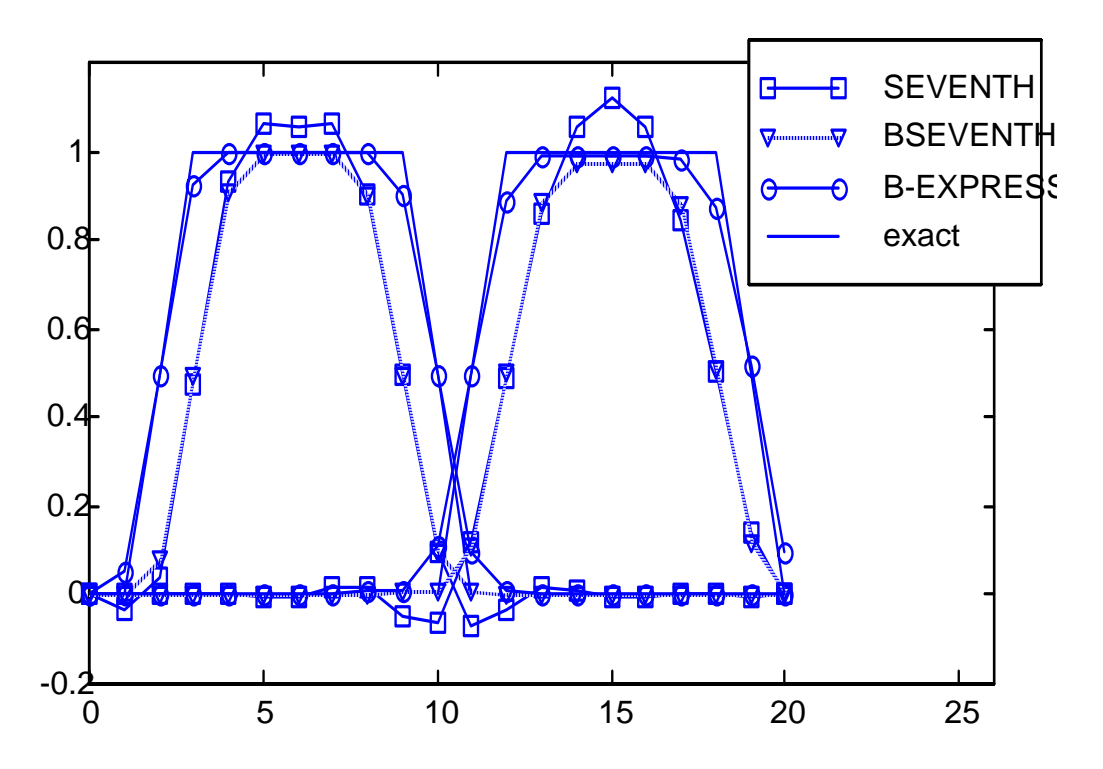


Figure 10: Convection of a double-step profile at x=0.25, x=0.75.

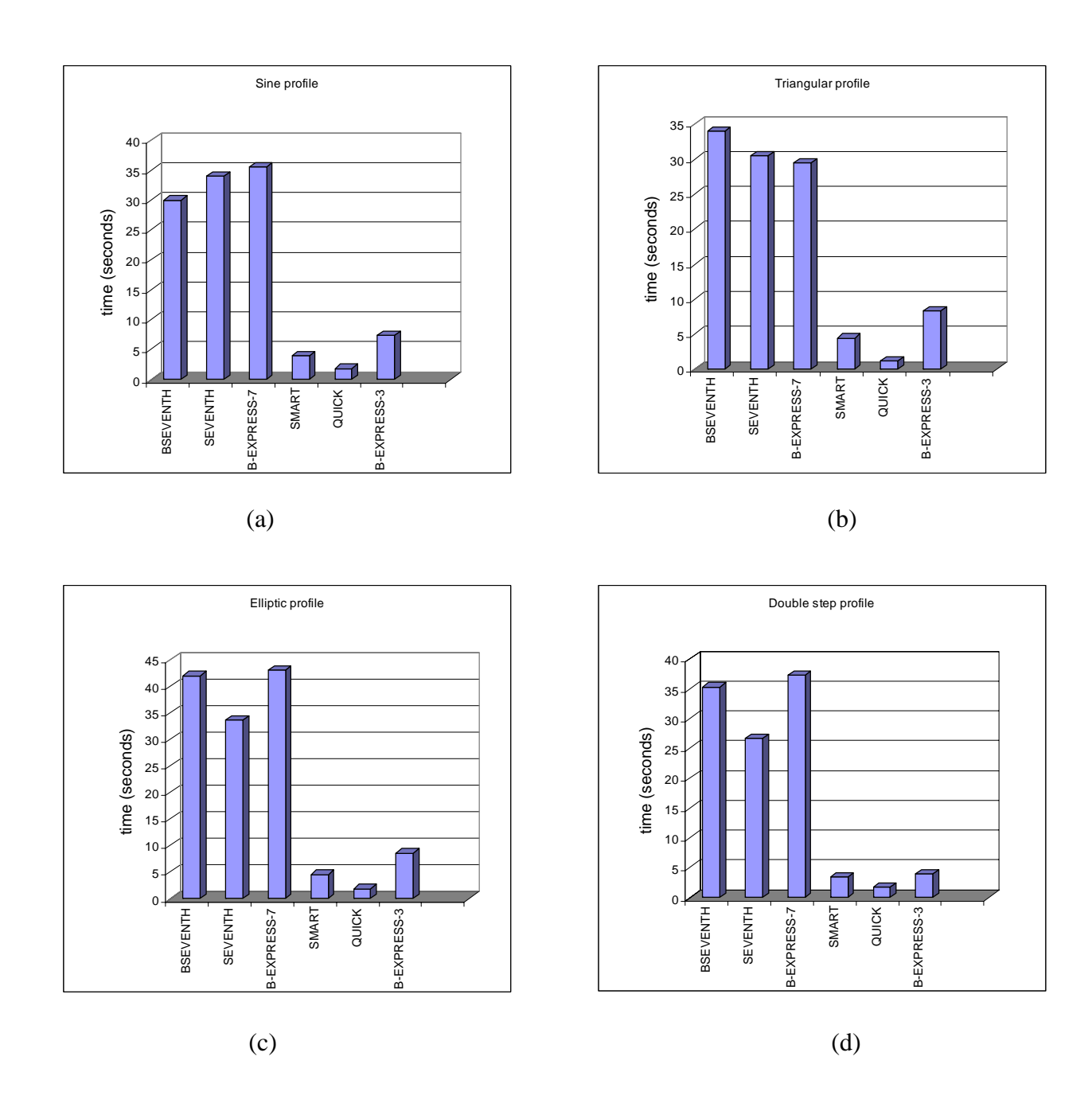


Figure 12: Time comparison for the convection in an oblique flow field of a (a) sine profile, (b) triangular profile, (c) elliptic profile, and (d) box profile.